

Hartree–Fock Orbital Instabilities and Symmetry-Breaking in ScO₂: Is a C_s Equilibrium Structure Viable?†

Seung-Joon Kim‡ and T. Daniel Crawford*

Department of Chemistry, Virginia Tech, Blacksburg, Virginia 24061

Received: October 6, 2003; In Final Form: January 8, 2004

We have applied high-level coupled cluster methods, in conjunction with a variety of reference molecular orbitals and basis sets, to consider the possibility that the equilibrium geometry of the ground state of ScO₂ breaks C_{2v} symmetry. The force constants for the antisymmetric stretching vibration (*b*₂ symmetry) have been computed across a domain of Sc–O bond distances and O–Sc–O bond angles at the spin-restricted open-shell Hartree–Fock (ROHF) and spin-unrestricted Hartree–Fock (UHF) levels of theory in order to investigate the importance of artifactual orbital instability envelopes on the properties computed with correlated wave functions. In most cases, Hartree–Fock instability regions are located far from the pertinent optimized geometries, suggesting that the corresponding harmonic vibrational frequencies should be free from artifactual orbital effects. Nevertheless, ROHF- and UHF-based coupled cluster models disagree qualitatively on the symmetry of ScO₂, and Brueckner orbital based methods give variable results with respect to basis set and level of electron correlation. Although full coupled cluster single-, double-, and triple-excitation results indicate symmetry breaking with smaller basis sets, extrapolation of the results to larger basis sets is inconclusive. The current results indicate with certainty only a flat symmetry-breaking potential. Furthermore, although all methods considered here predict that C_s optimized structures lie lower in energy than their C_{2v} counterparts, the highest levels of theory predict very low effective barriers to interconversion of equivalent C_s minima—low enough that the zero-point vibrational energy (even when computed with anharmonicity corrections) lies above the barrier leading to an overall *dynamical* C_{2v} symmetry.

I. Introduction

In a recent series of combined experimental–theoretical papers,^{1–3} Andrews, Bauschlicher, and co-workers examined the problematic ²B₂ ground state of scandium dioxide. In the first paper in 1997,¹ Chertihin et al. identified ScO₂ from the reaction of laser-ablated Sc atoms with molecular oxygen using matrix isolation infrared spectroscopy. Based in part on density-functional (DFT) calculations (specifically the BP86 functional in conjunction with a 6-31+G* basis for oxygen and a Wachters basis set for scandium), they assigned the observed 722 cm⁻¹ peak as the *b*₂-symmetry antisymmetric stretching fundamental frequency of ScO₂. However, they noted that the DFT predictions gave a lower than expected *ν*₃ value of 545 cm⁻¹ and that the B3LYP functional gave a structure with inequivalent Sc–O bonds (C_s symmetry). This work was followed in 1998 by a more detailed theoretical analysis in which they applied higher level *ab initio* models, including CASSCF and coupled cluster theories and larger basis sets (aug-cc-pVTZ for O and an averaged atomic natural orbital basis including up to *g*-type functions for Sc).² Their primary observations for ScO₂ were the following: (1) CASSCF and MP2 methods suffer from substantial orbital instability effects, leading to unphysical *b*₂ vibrational frequencies (>5000 cm⁻¹) and transition intensities (>99 999 km/mol); (2) the CCSD(T) approach (coupled cluster singles and doubles plus a perturbative estimate of connected triples) gives a *b*₂ frequency of 604 cm⁻¹, substantially lower

than the 722 cm⁻¹ experimental fundamental, but the computed ¹⁶O/¹⁸O isotopic shifts are in good agreement with the observed values.

In a third publication a year later, they reported new experimental and theoretical data.³ In particular, after doping the matrix with the electron-trapping species CCl₄, they found that the 722 cm⁻¹ vibrational band was dramatically reduced in intensity, suggesting that the carrier of the band was an anion. In addition, comparison to their new calculations at the density-functional, CCSD(T), and CASPT2 (CASSCF augmented by second-order perturbation theory) levels prompted reassignment of the 722 cm⁻¹ band to ScO₂⁻ (with an apparent negative anharmonicity of ca. 40 cm⁻¹). However, the mystery of the missing neutral ScO₂ vibrational bands remained, leading the authors to speculate that the equilibrium geometry could, in fact, be a symmetry-broken C_s structure. They further suggested that additional calculations involving varying reference functions (e.g., Brueckner orbitals) would be helpful in elucidating the significance of potential orbital instability effects in the coupled cluster approaches.

In a related study in 1998, Wu and Wang reported an analysis of the photoelectron spectrum of ScO₂⁻, in which they noted in passing that the *a*₁-symmetry *ν*₁ fundamental of ScO₂ was 740 cm⁻¹.⁴ Two years later, Gonzales, King, and Schaefer published an extensive theoretical study of the ground and several low-lying excited states of ScO₂⁻ and ScO₂.⁵ Although their coupled cluster results agreed well with the vertical detachment energy of ScO₂⁻ measured by Wu and Wang, instability effects in the spin-unrestricted (UHF) and spin-restricted (ROHF) orbitals prevented them from determining

† Part of the special issue "Fritz Schaefer Festschrift".

* Corresponding author. E-mail: crawdad@vt.edu.

‡ Permanent address: Department of Chemistry, HanNam University, Taejon 300-791, Korea.

CCSD(T) predictions for the problematic b_2 antisymmetric stretching frequency of ScO_2 neutral.

The purpose of this work is to further consider the possibility of a symmetry-broken equilibrium structure for the ground state of ScO_2 . In particular, we have applied high-level coupled cluster methods⁶ up to full CCSDT (coupled cluster singles, doubles, and triples) as well as a variety of reference determinants, including UHF, ROHF, and Brueckner-type orbitals, to investigate the impact of orbital instability effects on the harmonic vibrational frequencies. We find that, although CCSD(T) methods disagree on the shape of the Born–Oppenheimer potential along the b_2 antisymmetric stretching coordinate, full CCSDT results show much less deviation with respect to the choice of reference wave function. However, we find that the C_{2v} barrier separating equivalent C_s -symmetry structures is well below the zero-point vibrational energy, suggesting that it is unlikely the symmetry-broken structure is experimentally detectable.

II. Theoretical Approach

The structure and vibrational frequencies of ScO_2 were computed using high-level perturbation theory⁷ and coupled cluster methods:^{6,8–10} second-order many-body perturbation theory [MBPT(2)], coupled cluster singles and doubles (CCSD),¹¹ CCSD plus a perturbative estimate of connected triples [CCSD(T)],^{12,13} and full coupled cluster singles, doubles, and triples (CCSDT)^{14–16} in conjunction with spin-unrestricted Hartree–Fock (UHF), spin-restricted open-shell Hartree–Fock (ROHF), and Brueckner-type orbitals (defined as the set of molecular orbitals for which the single-excitation amplitudes are zero).^{17–20} Structural optimizations were carried out using analytic energy gradients at the UHF-²¹ and ROHF-based²² CCSD and CCSD(T) levels and at the B-CCD²⁰ levels of theory, and by finite differences of energies at the CCSDT and B-CCD(T) levels. Harmonic vibrational frequencies were computed using analytic energy second derivatives for the UHF-CCSD and UHF-CCSD(T) levels of theory,^{23–25} by finite differences of analytic gradients for ROHF-CCSD, ROHF-CCSD(T), and B-CCD, and by finite differences of energies for B-CCD(T) and CCSDT. In addition, UHF-CCSD(T) fundamental vibrational frequencies of C_s -symmetry ScO_2 were determined using second-order vibrational perturbation theory with cubic and semidiagonal quartic force constants computed via finite differences of analytic second derivatives using the method described by Stanton, Lopreore, and Gauss.²⁶ Excitation energies were computed using the equation-of-motion CCSD (EOM-CCSD) method.²⁷

For oxygen, the standard 6-31+G*²⁸ and aug-cc-pVTZ^{29,30} basis sets were used. For scandium, the (14s9p5d/8s4p3d) Wachters basis set was used, augmented by two sets of diffuse p-type and one set of diffuse d-type functions with orbital exponents $\alpha_p = 0.134\ 62$, $0.046\ 548$ and $\alpha_d = 0.0588$. The Wachters basis was further augmented by three sets of f-type functions, contracted to a single set to yield a final Sc basis of the form (41s11p6d3f/8s6p4d1f), hereafter labeled “Wachters+f”.^{31,32} All calculations were carried out with the ACESII program package.³³

III. Results and Discussion

A. Orbital Instability Regions and Force Constant Volcanoes. The unphysical and inconsistent predictions of harmonic vibrational frequencies described in previous theoretical studies of ScO_2 (e.g., CASSCF values in excess of $5000\ \text{cm}^{-1}$) can be the result either of “true” pseudo-Jahn–Teller interactions or

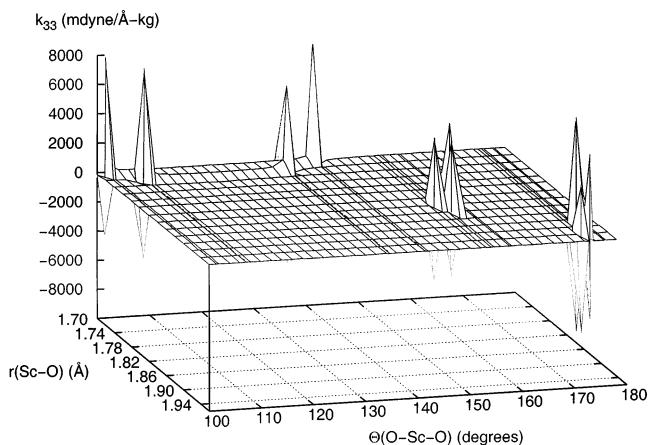


Figure 1. Plot of UHF quadratic force constant for b_2 antisymmetric stretching in 2B_2 ScO_2 as a function of Sc–O distance and O–Sc–O angle. The Wachters basis was used for scandium, and the 6-31+G* basis was used for oxygen.

of artifactual orbital instabilities arising from competing solutions to the Hartree–Fock or other appropriate orbital-defining equations.^{34–42} The latter problem manifests itself as near-zero eigenvalues of the molecular-orbital (MO) Hessian, the matrix of second derivatives of the Hartree–Fock energy with respect to nonredundant orbital rotations.^{34,35,41,43–49} The deleterious impact of such instabilities on highly correlated wave functions, such as those of coupled cluster theory, have been considered by Crawford et al.,⁴¹ who showed that quadratic force constants (and other second-order properties) depend quadratically on the derivatives of the orbital rotation parameters. Since these parameters are implicitly dependent upon the inverse of the MO Hessian [via the first-order coupled-perturbed Hartree–Fock (CPHF) equations], near singularity of the Hessian leads to anomalously large force constants and associated vibrational frequencies. The result is a “force constant volcano”, where the quadratic force constants plotted with respect to selected totally symmetric geometric coordinates exhibit second-order poles around a critical geometry. Crawford and co-workers showed empirically that the width of these volcanoes tends to be smaller for infinite-order coupled cluster methods, such as CCSD, than for perturbationally corrected methods, such as CCSD(T). Furthermore, for low-level methods such as MBPT(2)/MP2, the force constant volcanoes tend to be so large as to render such methods essentially useless for symmetry-breaking problems. Although for some years Brueckner methods were considered a cure-all for orbital instability problems (and artifactual symmetry-breaking problems, in general),^{36–38,40} more recent results indicate that this is not the case.⁴²

Figures 1 and 2 are plots of the UHF and ROHF quadratic force constants for the ScO_2 b_2 antisymmetric stretch as a function of the Sc–O distance and O–Sc–O angle (all C_{2v} geometries). These data were computed using the Wachters basis set for scandium (with no f-type functions) and the 6-31+G* basis set for oxygen, though additional calculations indicate that the structure of the force constant surface changes very little with larger basis sets. (Note that the finite peaks shown in the figures correspond to first-order poles with infinite values at the singularity.) The UHF force constants shown in Figure 1 reveal four primary singularity regions, corresponding to small-angle/short-bond, medium-angle/short-bond, medium-angle/medium-bond, and wide-angle/long-bond regions. Each singularity corresponds to a near-zero eigenvalue of the MO Hessian. If the optimized geometry of ScO_2 for a given correlated method, such as MBPT(2) or CCSD(T), lies close to one of these

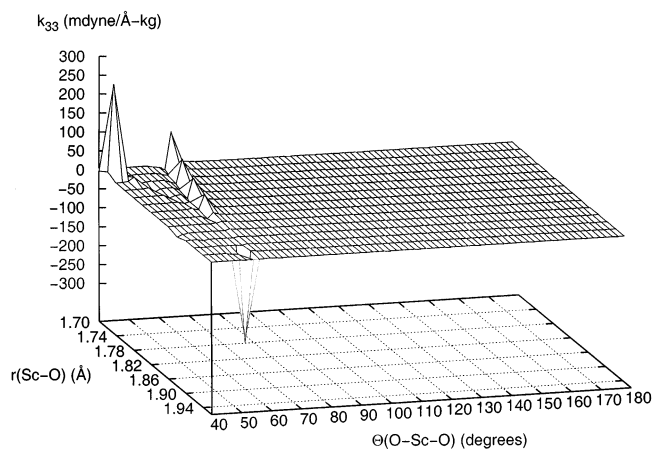


Figure 2. Plot of ROHF quadratic force constant for b_2 antisymmetric stretching in 2B_2 ScO₂ as a function of Sc–O distance and O–Sc–O angle. The Wachters basis was used for scandium, and the 6-31+G* basis was used for oxygen.

singularities, harmonic vibrational frequencies computed at the same level will have unphysically large values. Somewhat surprisingly, the ROHF force constants shown in Figure 2 reveal only two regions of orbital instability, and only for very small O–Sc–O angles, far from the expected equilibrium region of ca. 140° (vide infra). This suggests that MBPT or CC calculations based on an ROHF reference determinant are unlikely to be adversely affected by orbital instabilities, though it should be noted that this fact does not indicate the expected accuracy of the ROHF-based methods in describing true pseudo-Jahn–Teller interactions.

B. Structures and Harmonic Vibrational Frequencies.

Table 1 summarizes the molecular properties of the 2B_2 state ScO₂ computed at the MBPT(2), CCSD, CCSD(T), and full CCSDT levels of theory using the Wachters basis set for Sc and the 6-31+G* basis set for O. With these small basis sets, all four levels of theory agree reasonably well on the C_{2v} structure of the ground state, giving an Sc–O bond length of around 1.79 Å and an O–Sc–O bond angle of ca. 140°. [UHF-MBPT(2) is a notable dissenter, predicting a much shorter bond

length of 1.72 Å.] The methods disagree considerably, however, on the nature of the b_2 antisymmetric stretching frequency. UHF-MBPT(2) gives an obviously unphysical value for this mode of nearly 24 000i cm⁻¹. This result is consistent with Figure 1, which reveals a UHF orbital instability envelope in the vicinity of the UHF-MBPT(2) optimized structure, further evidence that low-level perturbative methods are worthless for symmetry-breaking problems. At the CCSD level, UHF and ROHF reference functions agree qualitatively (but not quantitatively) on a C_{2v} minimum-energy structure, but the Brueckner orbital approach predicts a strong imaginary b_2 vibration at 499i cm⁻¹. At the CCSD(T) level, UHF- and Brueckner-based methods now agree semiquantitatively on a C_s minimum, but ROHF-CCSD(T) still predicts C_{2v} symmetry. Finally, at the full CCSDT level, the ROHF- and UHF-based calculations agree on a symmetry-broken geometry. (B-CCDT calculations were not possible due to the size of the system and program limitations.) We also note that, although spin contamination in the UHF reference determinant is strong ($\langle \hat{S}^2 \rangle_{\text{UHF}} > 1.1$), the coupled cluster methods eliminate most of the effects of higher spin-multiplicity contributions (e.g., $\langle \hat{S}^2 \rangle_{\text{UHF-CCSD(T)}} = 0.756$).

Table 2 summarizes the properties of C_{2v} ScO₂ at the CCSD and CCSD(T) levels using the Wachters+f basis set on Sc, coupled with the 6-31+G* and aug-cc-pVTZ basis sets for O. The strong dependence of the predicted structure on the oxygen basis set is striking: with the smaller 6-31+G* basis, the O–Sc–O bond angle at the CCSD level is significantly widened with the UHF reference (159.8°) and is essentially linear with the ROHF and Brueckner references (174.1° and 180.0°, respectively). At the CCSD(T) level, however, these discrepancies disappear, and all reference functions predict an angle of approximately 145°. With the aug-cc-pVTZ basis set on oxygen, the CCSD methods again give a somewhat wider angle (ranging from 155° to 160°), while the CCSD(T) method consistently predicts ca. 149° with all three reference functions.

The most important results from Table 2, however, are the b_2 antisymmetric stretching frequencies. With UHF and ROHF references, the CCSD method gives a real frequency, indicating a C_{2v} minimum, though we note that the large-angle UHF-based

TABLE 1: Energies (E_h), Geometric Parameters (Å and deg), and Harmonic Vibrational Frequencies (cm⁻¹) for the 2B_2 State of ScO₂ at Various Levels of Theory with the 6-31+G* Basis for Oxygen and the Wachters Basis Set for Scandium

	UHF-MBPT(2)	UHF-CCSD	UHF-CCSD(T)	UHF-CCSDT ^a
energy	-910.173 956	-910.205 002	-910.232 613	-910.113 113
$r(\text{Sc-O})$	1.717	1.797	1.795	1.806
$\theta(\text{O-Sc-O})$	143.8	143.5	138.2	138.9
$\omega_1(a_1)$	1061	713	752	692
$\omega_2(a_1)$	147	127	124	116
$\omega_3(a_1)$	23939i	687	530i	137i
	ROHF-MBPT(2)	ROHF-CCSD	ROHF-CCSD(T)	ROHF-CCSDT ^a
energy	-910.234 404	-910.199 594	-910.233 715	-910.111 293
$r(\text{Sc-O})$	1.789	1.787	1.798	1.801
$\theta(\text{O-Sc-O})$	148.0	144.5	139.1	139.4
$\omega_1(a_1)$	746	744	721	713
$\omega_2(a_1)$	146	131	124	127
$\omega_3(a_1)$	1169	231	126	164i
		B-CCD	B-CCD(T)	
energy		-910.195 456	-910.234 887	
$r(\text{Sc-O})$		1.783	1.799	
$\theta(\text{O-Sc-O})$		145.4	138.7	
$\omega_1(a_1)$		752	722	
$\omega_2(a_1)$		132	126	
$\omega_3(a_1)$		499i	585i	

^a CCSDT results were computed with all core orbitals frozen.

TABLE 2: Energies (E_h), Geometric Parameters (\AA and deg), and Harmonic Vibrational Frequencies (cm^{-1}) for the 2B_2 State of ScO_2 at Various Levels of Theory with the Wachters+f Basis Set

	6-31+G*/O and Wachters+f/Sc		aug-cc-pVTZ/O and Wachters+f/Sc	
	UHF-CCSD	UHF-CCSD(T)	UHF-CCSD	UHF-CCSD(T)
energy	-910.240 307	-910.270 762	-910.438 019	-910.480 580
$r(\text{Sc}-\text{O})$	1.786	1.789	1.773	1.775
$\theta(\text{O}-\text{Sc}-\text{O})$	159.8	144.8	155.8	149.4
$\omega_1(a_1)$	724	735	740	746
$\omega_2(a_1)$	48	90	87	103
$\omega_3(a_1)$	1165	556i	1243	491i
	ROHF-CCSD	ROHF-CCSD(T)	ROHF-CCSD	ROHF-CCSD(T)
energy	-910.235 818	-910.271 536	-910.433 683	-910.481 760
$r(\text{Sc}-\text{O})$	1.780	1.790	1.767	1.777
$\theta(\text{O}-\text{Sc}-\text{O})$	174.1	146.1	157.5	149.6
$\omega_1(a_1)$	751	729	763	743
$\omega_2(a_1)$	9	86	82	101
$\omega_3(a_1)$	536	316	463	371
	B-CCD	B-CCD(T)	B-CCD	B-CCD(T)
energy	-910.231 386	-910.272 838	-910.430 113	-910.482 562
$r(\text{Sc}-\text{O})$	1.776	1.790	1.764	1.777
$\theta(\text{O}-\text{Sc}-\text{O})$	180.0	145.1	159.6	149.0
$\omega_1(a_1)$	760	721	769	738
$\omega_2(a_1)$	28	40	81	67
$\omega_3(a_1)$	242	409i	371i	3

results may be compromised due to the nearby orbital instability envelope at approximately $\theta(\text{O}-\text{Sc}-\text{O}) = 160^\circ$ and $r(\text{Sc}-\text{O}) = 1.80 \text{ \AA}$ (cf. Figure 1). The Brueckner orbital based CCD methods, however, are less consistent, predicting a C_{2v} minimum with the 6-31+G* basis set on oxygen and a C_s minimum with the aug-cc-pVTZ basis set. At the CCSD(T) level, the UHF- and Brueckner-based methods now agree on a symmetry-broken structure, though with the larger basis set the B-CCD(T) b_2 -symmetry frequency is too small (only 3 cm^{-1}) to draw any conclusions. [We note in passing that the flat B-CCD(T) potential for this mode required substantially tightened convergence criteria on both the coupled cluster wave function amplitudes (10^{-11} root-mean-square difference) and Brueckner orbital parameters (10^{-8} in the largest single-excitation amplitude). Nevertheless, due to the use of energy-based finite-difference procedures, this exceedingly small value can be precise only to within ca. $\pm 10 \text{ cm}^{-1}$.] The ROHF-based CCSD and CCSD(T) methods consistently predict a C_{2v} minimum-energy structure. It is also worth noting that the EOMIP-CCSD method (equation-of-motion CCSD method for ionized states),⁵⁰ which has been praised in the literature for its ability to correctly predict properties of radical species, gives a b_2 harmonic vibrational frequency of 593 cm^{-1} for ScO_2 with the aug-cc-pVTZ/O and Wachters+f/Sc basis sets.

The question remains, however, as to the importance of residual dynamic correlation effects: would the full CCSDT method with the larger basis set predict symmetry breaking regardless of reference determinant, as it did with the smaller basis sets (cf. Table 1)? If one assumes the trend from CCSD(T) to CCSDT with the small basis set holds for the larger basis set, one would expect that UHF-CCSDT, which shifts *upward* from $530i$ to $137i \text{ cm}^{-1}$ in Table 1, is likely to give an imaginary b_2 antisymmetric stretching frequency with the larger basis set, though it would probably be less than $100i \text{ cm}^{-1}$. The ROHF-CCSDT method, on the other hand, whose b_2 frequency shifts from 126 to $164i \text{ cm}^{-1}$ with the small basis set, would likely give a real frequency, again less than 100 cm^{-1} . The trend with the B-CCD(T) and B-CCDT methods, however, is less clear, because the shift from B-CCD to B-CCD(T) is inconsistent with respect to basis set.

TABLE 3: Excitation Energies (in eV) from the Ground 2B_2 State to the Lowest 2A_1 State of ScO_2 , Computed at the EOM-CCSD Level of Theory^a

ground-state geometry	${}^2B_2 \rightarrow {}^2A_1$ excitation energy
6-31+G*/O and Wachters/Sc	
UHF-CCSD	1.08
UHF-CCSD(T)	1.03
ROHF-CCSD	0.91
ROHF-CCSD(T)	0.81
6-31+G*/O and Wachters+f/Sc	
UHF-CCSD	1.27
UHF-CCSD(T)	1.09
ROHF-CCSD	2.30
ROHF-CCSD(T)	0.90
aug-cc-pVTZ/O and Wachters+f/Sc	
UHF-CCSD	1.30
UHF-CCSD(T)	1.00
ROHF-CCSD	2.16
ROHF-CCSD(T)	1.98

^a The ground-state geometry used is indicated on the left. In each case, the same reference wave function used for the geometry optimization was used with the EOM-CCSD approach.

We have also considered the potential for true pseudo-Jahn-Teller interactions, which, as stated earlier, are closely related to the orbital instability effects described above. Table 3 reports the EOM-CCSD excitation energies between the 2B_2 ground state and the lowest 2A_1 excited state, which may interact along the problematic antisymmetric stretching vibrational mode. The strength of the interaction between the states depends inversely on the excitation energy and directly on the vibronic (derivative) coupling parameter, leading to a first-order pole structure of the quadratic force constants along selected symmetry-preserving coordinates as the two states cross.^{51,52} As is clear from Table 3, the excitation energy is small, ranging from 0.81 eV for ROHF-EOM-CCSD at the ROHF-CCSD(T) level with the 6-31+G*/O and Wachters/Sc basis sets to 2.30 eV for ROHF-EOM-CCSD at the ROHF-CCSD level with the 6-31+G*/O and Wachters+f/Sc basis sets. The wide range of excitation energies stems from the corresponding variation in optimized structures (cf. Tables 1 and 2). However, no clear trend arises

TABLE 4: Absolute Energies (in E_h), Relative Energies (with Respect to the $C_{2v}^2B_2$ State, in kcal/mol), Geometric Parameters (Å and deg), and Harmonic Vibrational Frequencies (in cm^{-1}) for the $^2A'$ State of ScO₂ at Various Levels of Theory

	energy (ΔE)	$r(\text{Sc}-\text{O}_1)$	$r(\text{Sc}-\text{O}_2)$	$\theta(\text{O}-\text{Sc}-\text{O})$	ω_1	ω_2	ω_3
		6-31+G*/O and Wachters/Sc					
UHF-CCSD	-910.208 717 (-2.3)	2.009	1.697	124.0	962	157	523
ROHF-CCSD	-910.208 695 (-5.7)	2.009	1.697	124.0	962	157	523
UHF-CCSD(T)	-910.236 915 (-2.7)	1.997	1.715	121.4	910	150	495
ROHF-CCSD(T)	-910.236 922 (-2.0)	1.997	1.715	121.4	910	151	496
		6-31+G*/O and Wachters+f/Sc					
UHF-CCSD	-910.243 486 (-2.0)	1.996	1.692	123.9	969	155	540
ROHF-CCSD	-910.243 465 (-4.8)	1.996	1.692	123.9	969	154	540
UHF-CCSD(T)	-910.273 771 (-1.9)	1.983	1.709	121.0	915	147	515
ROHF-CCSD(T)	-910.273 779 (-1.4)	1.983	1.709	121.0	916	146	513
		aug-cc-pVTZ/O and Wachters+f/Sc					
UHF-CCSD	-910.441 146 (-2.0)	1.979	1.681	125.3	981	153	545
ROHF-CCSD	-910.441 096 (-4.7)	1.979	1.681	125.3	981	153	546
UHF-CCSD(T)	-910.481 756 (-0.7)	1.964	1.698	123.0	930	141	505
ROHF-CCSD(T)	-910.481 790 (-0.02)	1.964	1.698	123.1	930	136	507

relating the size of the excitation energy to the magnitude of the b_2 antisymmetric stretching frequency. This is not surprising, however, given the fact that truncated coupled cluster methods do not reproduce the “true” pseudo-Jahn–Teller interaction pole structure, and the lower states of an interacting pair may even exhibit increased curvature in the presence of strong interactions. As a result, such data cannot be used to distinguish between real vs artifactual pseudo-Jahn–Teller behavior. This point has been addressed in detail recently by Stanton⁵¹ and by Russ and Crawford.⁵²

To consider the question of a viable C_s minimum-energy structure further, we have also explicitly optimized broken-symmetry structures with the UHF and ROHF reference functions; these are reported in Table 4. Unlike the C_{2v} -symmetry results in Tables 1 and 2, the C_s -symmetry data are consistent with respect to the choice of reference orbitals. For a given basis set, the UHF- and ROHF-based coupled cluster methods agree extremely well for all properties considered here. Perhaps the most interesting results from Table 4 are the relative energies with respect to the corresponding C_{2v} optimized structures. In every case, the C_s structure is predicted to lie lower than its C_{2v} counterpart, even for those methods which predict a real b_2 vibrational frequency at the C_{2v} structure [e.g., ROHF-CCSD(T)]. These results are consistent with those reported by Bauschlicher and co-workers.³

Do these results indicate that the global minimum for the ground state of ScO₂ is a C_s symmetry-broken structure? The UHF-CCSD(T) and ROHF-CCSD(T) results computed with the aug-cc-pVTZ/O and Wachters+f/Sc basis sets are the linchpin. (1) For the C_{2v} structure both methods predict a flat b_2 antisymmetric stretching potential, though they differ in the sign of the curvature; (2) both methods predict a very shallow C_s -symmetry well: UHF-CCSD(T) predicts that the C_{2v} barrier is only 0.7 kcal/mol above the C_s double-well minima, and ROHF-CCSD(T) predicts a 0.02 kcal/mol difference between its C_{2v} and C_s minima. The zero-point vibrational energies for both methods, on the other hand, are approximately 2.2 kcal/mol (778 cm^{-1}), well above these barriers.

To investigate the possibility that anharmonic corrections, which typically lower the zero-point vibrational energy, could stabilize the C_s minima, we have also computed anharmonicity corrections to the UHF-CCSD(T) frequencies with the 6-31+G*/O and Wachters/Sc basis sets using second-order vibrational perturbation theory.²⁶ The correction for each frequency is small and negative: $\nu_1 = 895$, $\nu_2 = 146$, and $\nu_3 = 468$ cm^{-1} , leading to a zero-point energy of 770 cm^{-1} , only 8 cm^{-1} below the zero-point vibrational energy computed using

harmonic frequencies. Thus, while the Born–Oppenheimer potential may indeed exhibit a double-well potential around the C_{2v} central point, it is unlikely that the C_s symmetry structures can be identified experimentally. The structure inferred from experimental rotational fine structure, for example, would correspond to an average of the bond lengths reported in Table 4.

IV. Conclusions

We have used high-level coupled cluster methods, in conjunction with a variety of reference molecular orbitals and basis sets, to consider the viability of a broken-symmetry C_s equilibrium geometry for the ground state of ScO₂. Orbital instability effects compromise the accuracy of some of the UHF-based coupled cluster data, but for most of the calculations, the variation from level to level is the result of varying descriptions of a true pseudo-Jahn–Teller interaction. Full CCSDT calculations with smaller basis sets predict that the C_{2v} -symmetry optimized geometry is a transition state along the b_2 antisymmetric stretching potential, but extrapolation of these results to larger basis sets is inconclusive. The current results can indicate with certainty only a flat symmetry-breaking potential, with indefinite sign. Furthermore, although all methods considered here predict that C_s optimized structures lie lower in energy than their C_{2v} counterparts, the highest levels of theory predict very low effective barriers to interconversion of equivalent C_s minima—low enough that the zero-point vibrational energy lies above the barrier leading to an overall *dynamical* C_{2v} symmetry.

Acknowledgment. This work was supported by a CAREER award from the National Science Foundation (CHE-0133174) and a New Faculty Award from the Camille and Henry Dreyfus Foundation.

References and Notes

- (1) Chertihin, G. V.; Andrews, L.; Rosi, M.; Bauschlicher, C. W. *J. Phys. Chem. A* **1997**, *101*, 9085–9091.
- (2) Rosi, M.; Bauschlicher, C. W.; Chertihin, G. V.; Andrews, L. *Theor. Chim. Acta* **1998**, *99*, 106–112.
- (3) Bauschlicher, C. W.; Zhou, M.; Andrews, L.; Johnson, J. R. T.; Panas, I.; Snis, A.; Roos, B. O. *J. Phys. Chem. A* **1999**, *103*, 5463–5467.
- (4) Wu, H.; Wang, L.-S. *J. Phys. Chem. A* **1998**, *102*, 9129–9135.
- (5) Gonzales, J. M.; King, R. A.; Schaefer, H. F. *J. Chem. Phys.* **2000**, *113*, 567–572.
- (6) Crawford, T. D.; Schaefer, H. F. In *Reviews in Computational Chemistry*; Lipkowitz, K. B., Boyd, D. B., Eds.; VCH Publishers: New York, 2000; Vol. 14, Chapter 2, pp 33–136.
- (7) Bartlett, R. J. *Annu. Rev. Phys. Chem.* **1981**, *32*, 359.

- (8) Bartlett, R. J. In *Modern Electronic Structure Theory*; Yarkony, D. R., Ed.; Advanced Series in Physical Chemistry 2; World Scientific: Singapore, 1995; Chapter 16, pp 1047–1131.
- (9) Lee, T. J.; Scuseria, G. E. In *Quantum Mechanical Electronic Structure Calculations with Chemical Accuracy*; Langhoff, S. R., Ed.; Kluwer Academic Publishers: Dordrecht, 1995; pp 47–108.
- (10) Gauss, J. In *Encyclopedia of Computational Chemistry*; Schleyer, P., Ed.; Wiley: New York, 1998.
- (11) Rittby, M.; Bartlett, R. J. *J. Phys. Chem.* **1988**, *92*, 3033.
- (12) Raghavachari, K.; Trucks, G. W.; Pople, J. A.; Head-Gordon, M. *Chem. Phys. Lett.* **1989**, *157*, 479.
- (13) Bartlett, R. J.; Watts, J. D.; Kucharski, S. A.; Noga, J. *Chem. Phys. Lett.* **1990**, *165*, 513; erratum: **1990**, *167*, 609.
- (14) Hoffmann, M. R.; Schaefer, H. F. *Adv. Quantum Chem.* **1986**, *18*, 207.
- (15) Noga, J.; Bartlett, R. J. *J. Chem. Phys.* **1987**, *86*, 7041; erratum **1988**, *89*, 3401.
- (16) Watts, J. D.; Bartlett, R. J. *J. Chem. Phys.* **1990**, *93*, 6104.
- (17) Nesbet, R. K. *Phys. Rev.* **1958**, *109*, 1632.
- (18) Chiles, R. A.; Dykstra, C. E. *J. Chem. Phys.* **1981**, *74*, 4544.
- (19) Stolarczyk, L. Z.; Monkhorst, H. J. *Int. J. Quantum Chem. Symp.* **1984**, *18*, 267.
- (20) Handy, N. C.; Pople, J. A.; Head-Gordon, M.; Raghavachari, K.; Trucks, G. W. *Chem. Phys. Lett.* **1989**, *164*, 185.
- (21) Gauss, J.; Stanton, J. F.; Bartlett, R. J. *J. Chem. Phys.* **1991**, *95*, 2623.
- (22) Gauss, J.; Lauderdale, W. J.; Stanton, J. F.; Watts, J. D.; Bartlett, R. J. *Chem. Phys. Lett.* **1991**, *182*, 207.
- (23) Gauss, J.; Stanton, J. F. *Chem. Phys. Lett.* **1997**, *276*, 70.
- (24) Stanton, J. F.; Gauss, J. In *Recent Advances in Coupled-Cluster Methods*; Bartlett, R. J., Ed.; World Scientific Publishing: Singapore, 1997; pp 49–79.
- (25) Szalay, P. G.; Gauss, J.; Stanton, J. F. *Theor. Chim. Acta* **1998**, *100*, 5–11.
- (26) Stanton, J. F.; Lopreore, C. L.; Gauss, J. *J. Chem. Phys.* **1998**, *108*, 7190–7196.
- (27) Stanton, J. F.; Bartlett, R. J. *J. Chem. Phys.* **1993**, *98*, 7029.
- (28) Hariharan, P. C.; Pople, J. A. *Theor. Chim. Acta* **1973**, *28*, 213–222.
- (29) Dunning, T. H. *J. Chem. Phys.* **1989**, *90*, 1007.
- (30) Kendall, R. A.; Dunning, T. H.; Harrison, R. J. *J. Chem. Phys.* **1992**, *96*, 6796.
- (31) Wachters, A. J. *Chem. Phys.* **1970**, *52*, 1033.
- (32) Bauschlicher, C.; Langhoff, S.; Barnes, L. *J. Chem. Phys.* **1989**, *91*, 2399.
- (33) Stanton, J. F.; Gauss, J.; Watts, J. D.; Lauderdale, W. J.; Bartlett, R. J. *ACESII*; 1993. The package also contains modified versions of the MOLECULE Gaussian integral program of J. Almlöf and P. R. Taylor, the ABACUS integral derivative program written by T. U. Helgaker, H. J. Aa. Jensen, P. Jørgensen, and P. R. Taylor, and the PROPS property evaluation integral code of P. R. Taylor.
- (34) Allen, W. D.; Horner, D. A.; DeKock, R. L.; Remington, R. B.; Schaefer, H. F. *Chem. Phys.* **1989**, *133*, 11–45.
- (35) Burton, N. A.; Yamaguchi, Y.; Alberts, I. L.; Schaefer, H. F. *J. Chem. Phys.* **1991**, *95*, 7466.
- (36) Stanton, J. F.; Gauss, J.; Bartlett, R. J. *J. Chem. Phys.* **1992**, *97*, 5554.
- (37) Barnes, L. A.; Lindh, R. *Chem. Phys. Lett.* **1994**, *223*, 207–214.
- (38) Xie, Y.; Allen, W. D.; Yamaguchi, Y.; Schaefer, H. F. *J. Chem. Phys.* **1996**, *104*, 7615.
- (39) Hrušák, J.; Iwata, S. *J. Chem. Phys.* **1997**, *106*, 4877.
- (40) Crawford, T. D.; Stanton, J. F.; Szalay, P. G.; Schaefer, H. F. *J. Chem. Phys.* **1997**, *107*, 2525.
- (41) Crawford, T. D.; Stanton, J. F.; Allen, W. D.; Schaefer, H. F. *J. Chem. Phys.* **1997**, *107*, 10626.
- (42) Crawford, T. D.; Stanton, J. F. *J. Chem. Phys.* **2000**, *112*, 7873.
- (43) Čížek, J.; Paldus, J. *J. Chem. Phys.* **1967**, *47*, 3976.
- (44) Paldus, J.; Čížek, J. *Chem. Phys. Lett.* **1969**, *3*, 1.
- (45) Paldus, J.; Čížek, J. *J. Chem. Phys.* **1970**, *52*, 2919.
- (46) Paldus, J.; Čížek, J. *J. Chem. Phys.* **1971**, *54*, 2293.
- (47) Paldus, J.; Čížek, J. *Can. J. Chem.* **1985**, *63*, 1803.
- (48) Deguchi, K.; Nishikawa, K.; Aono, S. *J. Chem. Phys.* **1981**, *75*, 4165.
- (49) Yamaguchi, Y.; Alberts, I. L.; Goddard, J. D.; Schaefer, H. F. *Chem. Phys.* **1990**, *147*, 309.
- (50) Stanton, J. F.; Gauss, J. *J. Chem. Phys.* **1994**, *101*, 8938.
- (51) Stanton, J. *J. Chem. Phys.* **2001**, *115*, 10382–10393.
- (52) Russ, N. J.; Crawford, T. D. *J. Chem. Phys.*, in press.